Combustion and Flame 275 (2025) 113994

Contents lists available at ScienceDirect

Combustion and Flame

journal homepage: www.sciencedirect.com/journal/combustion-and-flame

Role of anions in the electrochemical modulation of flammability of ionic liquids

Afrida Anis, Keren Shi, Erik Hagen, Yujie Wang, Prithwish Biswas, Michael R. Zachariah *

University of California, Riverside, United States

ARTICLE INFO

Keywords:
Volatility, Flammability
Modulation
Anion
Inhibition

ABSTRACT

The flammability and combustion of liquid fuels is very dependent on volatility. Although room temperature ionic liquids (RTILs) without metastable anions possess high energy density, they are often considered non-flammable due to their low vapor pressure. We have demonstrated that these thermally stable and seemingly non-flammable imidazole cation based RTILs without metastable anions can be made flammable by applying a voltage bias which generates volatile flammable gaseous species. Conversely removing the voltage bias terminates the generation of these gaseous species, rendering the liquid non-flammable again. Utilizing this concept, we extend our study to investigate the effect of different anions BF_4^-, ClO_4^-, NO_3^-, PF_6^- and CH_3COO^-, paired with the same 1-butyl-3-methylimidazolium cation. We find that the rate of gaseous species generation largely depends on the conductivity of the RTILs. RTIL with higher conductivity produces more gaseous species. However, we also found that despite generating reactive gaseous species, some RTILs can still remain non-flammable. Mass spectrometric analysis of the gaseous species generated during the electrochemical decomposition shows that if the species generated from anodic oxidation possess flame inhibition properties, they can interfere with the combustion of the flammable species generated at the cathode, making them non-flammable. Flammability of other RTILs that do not have inhibiting species generated at the anode can be modulated electrochemically.

1. Introduction

High energy density liquid hydrocarbon fuels burn in the gas phase, and thus their flammability is directly related to their vapor pressure. This can lead to safety concerns regarding unintended ignition and explosion and may often require specialized storage. Liquid hydrocarbon fuels combust in the vapor phase and achieve self-sustained combustion through the heat feedback from the flame, which vaporizes sufficient liquid fuel required for the steady burning [1–3]. Extinction of the flame then requires removal of oxidant, which is typically, air.

An alternative approach for flame modulation, that has been gaining recent interest is electrical control, for example electrically controlled solid propellants (ECSP) and gel propellants (ECGP), can be manipulated through electrical means to control ignition, and throttling burn rate [4]. Several studies on ECSPs have found that to manipulate the combustion velocity, a liquid melt layer must first be created through the thermal decomposition of the ECSP constituents [4–6]. This is because ions can move more easily through liquid than solid. Creating this melt layer often requires a substantially high voltage, exceeding 100 Vs, to facilitate the decomposition through ohmic heating [4]. This also suggests that a liquid could be modulated more efficiently since the creation of a melt layer is not required. Herein we turn our attention to another class of energetic material, non-flammable room temperature ionic liquids (RTILs), since in our last study we found that the combustion of RTILs can be switched on/off when desired and their flame can be extinguished by simple removal of the voltage bias.

Room temperature ionic liquids (RTILs) are defined as salts with melting points below 100 °C. RTILs are also regarded as a special class of hydrocarbons with extremely low vapor pressure and superior thermal stability which reduces the likelihood of generating reactive gaseous species [7–11]. As a result, they are often considered 'non-flammable' [12–15]. However, most room temperature ionic liquids (RTILs) potentially possess high energy density and are often referred to as 'energetic ionic liquids' (EILs) and regarded as a new generation of high energy density (HED) hypergolic fuels [16]. Such high energy density fuels have generated interest for propulsion applications [17]. While

* Corresponding author.
E-mail address: mrz@engr.ucr.edu (M.R. Zachariah).

https://doi.org/10.1016/j.combustflame.2025.113994
Received 18 August 2024; Received in revised form 8 January 2025; Accepted 17 January 2025
Available online 21 February 2025

energetic ionic liquids with metastable anions like azides, dinitramides, borohydrides, and azoles can thermally or hypergolically decompose to reactive flammable species, other RTILs without these reactive anions are quite thermally stable and need other routes to be activated [18–23]. This suggests that the constituent anion has a significant role and is the subject of this paper. In particular, we found that thermally stable RTILs can be manipulated through an electrochemical approach making a non-flammable RTIL flammable [24]. We showed that the aromaticity of the imidazole ring of the apparent thermally stable and nonflammable imidazole based ionic liquids can be broken electrochemically resulting in the volatilization of the RTILs as reactive flammable species which can be ignited to create a stable flame. In Fig. 1 the proposed mechanism of electrochemical decomposition of the imidazole based ionic liquids at the electrodes is presented.

Furthermore, the removal of voltage bias will terminate this electrochemical reaction and consequently halt the generation of volatile species resulting in flame extinction [24]. This process can be repeated to undergo ignition – extinction as a tool to control or throttle the process.

In this study we show that the electrochemical modulation of the flammability of the room temperature ionic liquids largely depend on the anions. We demonstrate this with five imidazole based RTILs: 1-butyl 3-methyl imidazolium perchlorate ($[BMIM]^+[ClO_4]^-$),1-butyl 3-methyl imidazolium nitrate ($[BMIM]^+[NO_3]^-$), 1-butyl 3-methyl imidazolium acetate ($[BMIM]^+[CH_3COO]^-$) or ($[BMIM]^+[Ac]^-$),1-butyl 3-methyl imidazolium tetrafluoroborate ($[BMIM]^+[BF_4]^-$), 1-butyl 3-methyl imidazolium hexafluorophosphate ($[BMIM]^+[PF_6]^-$) all of which have the same organic imidazole cation but different anions. The most common cations used in applications such as solvent extraction, synthesis are based on imidazolium or pyridinium ring with one or more alkyl chain attached to it and typical anions are halogenated or oxygenated inorganic or organic anions [25,26]. So, we chose a combination of inorganic and organic anions attached to the same alkyl imidazolium cation in this study. To compare the generation of gaseous species among five imidazole ionic liquids, we measured the current produced during their respective electrochemical reactions and correlated it to the surface reaction rate. We initially hypothesized that the ionic liquid with the highest generation rate would be the most combustible. However, this study revealed that the nature of the anion is critical to determining flammability.

2. Experimental section

2.1. Materials

$[BMIM]^+[Cl]^-$ (~98 %) solid powder (m.p. ~70°C) were procured from Sigma Aldrich. Anhydrous $NaClO_4$ crystals, ACS, 98–102 % were bought from Thermo scientific, potassium acetate, ACS, ≥99 % was bought from Sigma Aldrich, crystalline sodium nitrate, $NaNO_3$ and solvents such as ethanol and dichloromethane were obtained from Fischer scientific. Two of the ionic liquids $[BMIM]^+[BF_4]^-$ (≥98 %) and $[BMIM]^+[PF_6]^-$ (≥97 % HPLC) were bought from Sigma Aldrich, rest of the three were synthesized in the laboratory. Molecular Sieves, 0.3 nm, were bought from Sigma Aldrich.

2.2. RTIL preparation

Five imidazolium based RTILs were used in this study, in which the cation was kept constant, and the anion was varied. This approach was predicated on our previously reported result that the imidazole ring decomposes at the cathode and produces flammable gaseous species. The type of imidazole ring did not seem to affect the flammability much, but we believe the anions might as the oxidation products will be different [24]. The five chosen anions are: BF_4^-, ClO_4^-, NO_3^-, PF_6^-, CH_3COO^-. These were chosen due to ready availability, and a mix of fluorine and oxygen based anions.1-butyl 3-methyl imidazolium perchlorate ($[BMIM]^+[ClO_4]^-$),1-butyl 3-methyl imidazolium nitrate ($[BMIM]^+[NO_3]^-$),1-butyl 3-methyl imidazolium acetate ($[BMIM]^+[CH_3COO]^-$) or ($[BMIM]^+[Ac]^-$),which were synthesized by the hard acid soft base anion exchange method by reacting dissolved precursors $[BMIM]^+[Cl]^-$ and $NaClO_4$ to produce $[BMIM]^+[ClO_4]^-$, $[BMIM]^+[Cl]^-$ and $NaNO_3$ to produce $[BMIM]^+[NO_3]^-$, $[BMIM]^+[Cl]^-$ and CH_3COOK to produce $[BMIM]^+[Ac]^-$. More details on the synthesis of $[BMIM]^+[ClO_4]^-$ can be found on our previous work and information about synthesis of $[BMIM]^+[NO_3]^-$ and $[BMIM]^+[Ac]^-$ can be found in Section S.1 in the supporting information [24]. All the ionic liquids were treated with 0.3 nm molecular sieve and kept in vacuum dryer for at least 24 h for further purification prior to each experiment.

2.3. Electrochemical measurements

For the electrochemical studies we fabricated a cell with VeroUltra

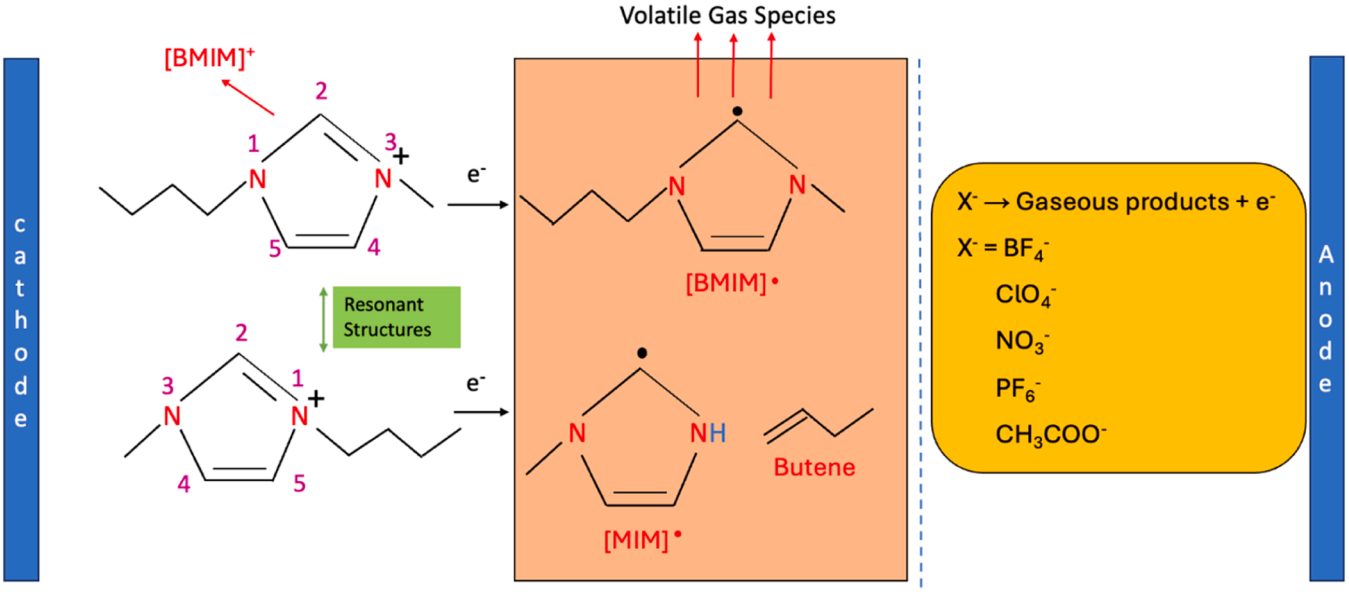

Fig. 1. Electrochemical decomposition of imidazole cation based RTILs with different anions.

WhiteS shown in Fig. 2 with dimensions of 25mm×25mm×3mm. The cell has through holes for inserting the electrodes and has supports for attaching the platinum wire electrodes so that they remain fixed. The platinum electrodes at one side of the cell were connected to the power source for applying the DC voltage bias. Current was measured with a Hewlett Packard 34401A digital multimeter, and for the linear sweep voltammetry measurements we used an AMEL 2553 high voltage potentiostat-galvanostat.

2.4. Linear sweep voltammetry

To determine the voltage window where the ionic liquids remain stable (i.e. no electrolysis) we used linear sweep voltammetry (LSV). LSV is an electrochemical technique that involves a single sweep from a lower potential limit to a higher potential limit at a specified voltage scan rate [27]. We chose linear sweep voltammetry because we are not concerned with the reversibility of the system. In two electrodes setup, the electrodes are connected to a potentiostat and immersed in the electrolyte (ionic liquid). The potentiostat controls the potential between the working and counter electrodes and measures the current to generate an I-V polarization curve [27]. This curve illustrates the oxidation and reduction responses of the electrolyte. A sharp change in the polarization curve indicates where oxidation or reduction begins. By identifying the difference between the onset of these peaks, we can determine the stable voltage range of the ionic liquid electrolyte.

2.5. Time of flight mass spectrometry of RTILs

To understand the nature of the volatile species generated during the electrochemical reactions, in-situ electrochemical mass spectrometry was conducted under vacuum conditions. To do this an approximately 0.05 ml of sample was placed on a glass slide with two ~75 μm diameter Pt wire electrodes immersed in it. The assembly was connected to the terminals of the same DC power supply as described in the previous section and was inserted the into the high vacuum ($\sim 10^{-9}$ atm) chamber of a time-of-flight mass spectrometer, between the ion extraction and repeller plate of the time- of-flight assembly. The gas phase species generated on electrolysis were ionized at ~70 eV by electron impact. Spectra were obtained at 10 kHz for a total during of 100ms. More details about the working principle of the time-of-flight component of this characterization can be found elsewhere [28,29].

2.6. Combustion and cyclability of ionic liquids

To demonstrate the combustion behavior under electrochemical activation, 0.00185 mol of ionic liquid was placed in the cavity of the electrochemical cell (Fig. 2). When exposed to a butane torch no ignition or sustained combustion is observed, indicating the RTILs are non-flammable. However, when the power source is turned on beyond the stable range of the ionic liquids (determined from linear sweep voltammetry), the ionic liquids begin decomposing as evidenced by bubbling and gas generation. Now under exposure to an ignition source (butane torch), a steady flame is generated, as exampled in Fig. 3, demonstrating electrochemical activation. Upon removal of the voltage, the flame will extinguish, and this cycle can be repeated. All the combustion events of the ionic liquids were captured with a Phantom Miro M110 high speed color camera with a Nikon 105 mm f/2.8 AF micro lens. All videos were recorded at 832×800 pixels with f/2.8. Other camera settings can be found in the supplementary section.

2.7. Temperature measurement by IR imaging

To measure the spatial surface temperature distribution during electrolysis a Telops, FAST M3 K IR camera was used. Videos were recorded with a 50 mm lens with 0.5-inch extension ring using a 10 μs exposure time, at 100 Hz and a resolution of 105 μm per pixel.

3. Results and discussion

3.1. Electrochemical potential window

For many applications, particularly as electrolytes in batteries and supercapacitors, RTILs are attractive for their superior electrochemical and thermal stability, alongside their ability to enhance the mobility of the solvated ions actively participating in the electrochemical reaction. In contrast, our major focus is on understanding the role of the thermodynamic activation barrier, ionic, and self-diffusivity of pure phase RTILs, in controlling the rate of generation of flammable species through their direct electrolysis. The electrochemical potential window (EPW) is a generic measure of the activation barrier to the electrolysis of different electrolytes. The EPW is defined as the difference between the oxidation onset potential and reduction onset potential, which are determined from the I-V polarization curves obtained through voltammetry. A characteristic electrochemical I-V curve can be segregated into two separate zones i) capacitive current zone: below the activation voltage of the redox reaction, a minor increase in current with voltage is observed

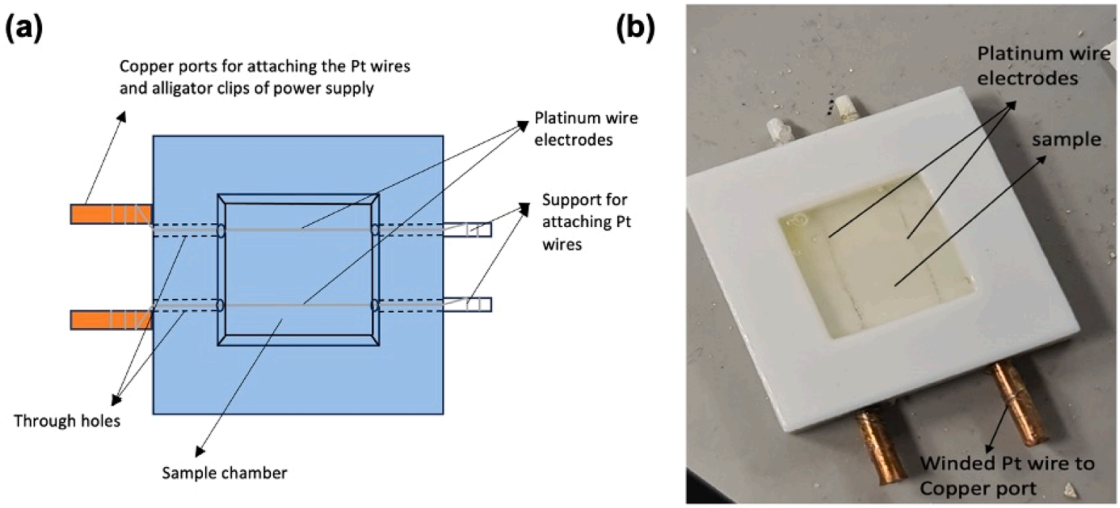

Fig. 2. (a) Schematic of the customized electrochemical cell (b) snapshot of the electrochemical cell.

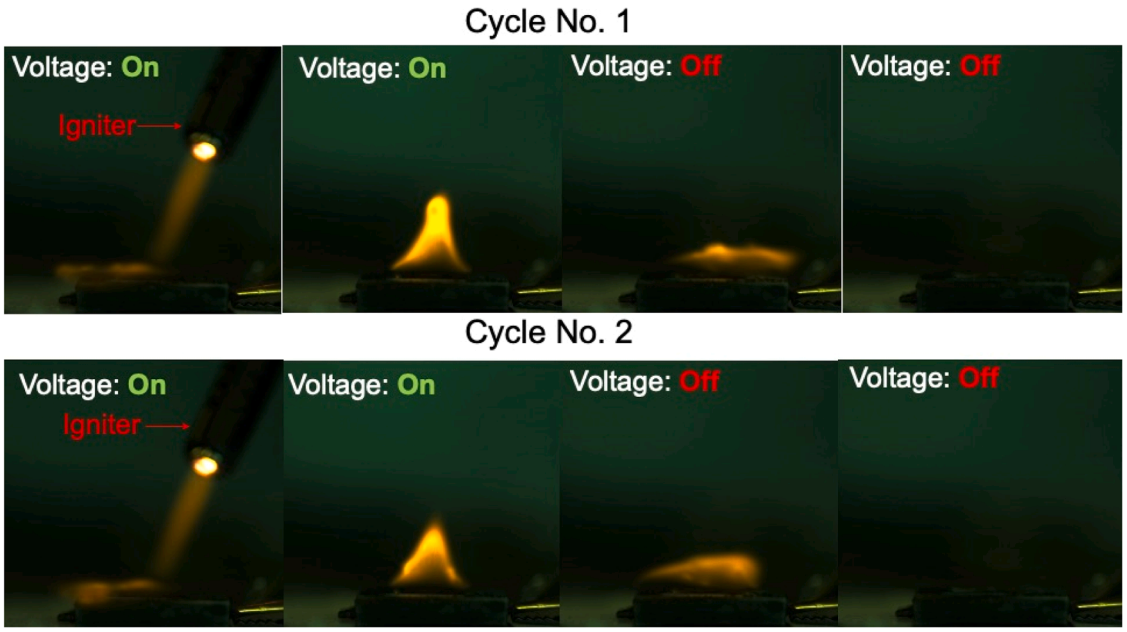

Fig. 3. Electrochemical activation and deactivation of the combustion of room temperature ionic liquid, $[BMIM]^+[Ac]^-$ at 20 V.

due to initial ionic charge accumulation near the electrode ii) Faradaic current zone: above the activation voltage, current continuously increases non-linearly with increasing voltage as more ions drift towards the electrodes. For most electrochemical applications, all electrolytes are used within the first zone, but we are interested in the second zone for RTIL fuels.

We obtained the I-V curve via linear sweep voltammetry measurements using a two-electrode system (working and counter) rather than the more traditional three electrodes system. Since the working electrode potential is now no longer defined against a standard electrode potential, the EPW measured might be different than the literature, as it depends on factors such as electrode material and electrode configuration [30–32].

The linear sweep voltammetry measurement in Fig. 4 shows that of the five RTIL's, $[BMIM]^+[PF_6]^-$ has the widest EPW of ~9.6 V, and

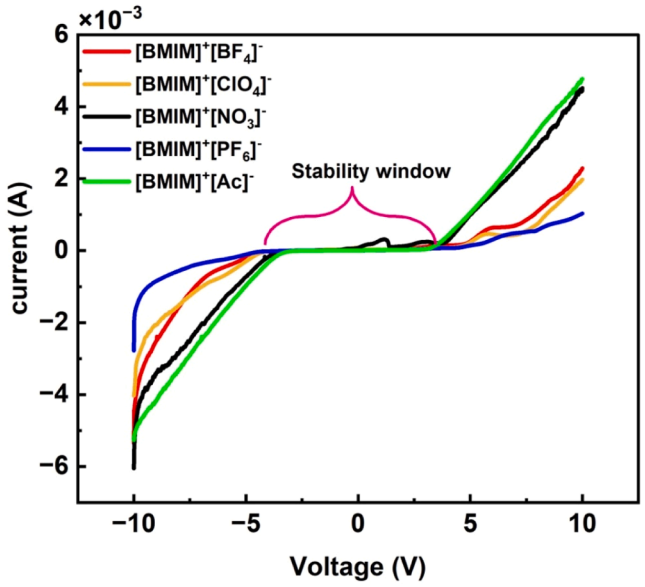

Fig. 4. Linear sweep voltammetry of the electrochemical stability window of RTILs.

$[BMIM]^+[Ac]^-$ the smallest, ~6.4 V. The stability is in the order $[BMIM]^+[PF_6]^-$ > $[BMIM]^+[BF_4]^-$ > $[BMIM]^+[ClO_4]^-$ > $[BMIM]^+[NO_3]^-$ > $[BMIM]^+[Ac]^-$. In the work of Kazemiabnavi et al., they have compared the oxidation potential of various anions and anions with lowest HOMO (Highest occupied molecular orbital) are expected to have the higher oxidation potential, owing to the higher energy gap between the low HOMO of the anion and the Fermi level (E_F) of the electrode. Usually, molecules or ions consisting of electronegative atoms have low HOMO levels and hence fluorinated species such as PF_6^- and BF_4^- need a higher activation potential to overcome the energy gap between their HOMO level and E_F of anode [33]. The oxidation potentials of the other oxygenated anions in our study vary due to the extent of charge delocalization between the constituent atoms [34]. From Fig. 4 we can see that despite having the same cation, the reduction potential of the cation in fact differs from each other, possibly due to differences in ion-ion interactions [35]. Although the exact voltages measured here may differ from that seen in other works due to differences in experimental configurations, the order of measured electrochemical stability aligns with the literature [36].

3.2. Electrochemical decomposition behavior of RTILs

Fig. 1 outlined the proposed mechanism of the electrochemical decomposition of imidazole ionic liquids to generate volatile reactive gas species. We now turn to measurement of the generation rate of such species at specified applied biases of 15 V and 20 V since these voltage biases are beyond the stability window of RTILs observed in Fig. 4.

In Fig. 5 we show the temporal variation of the reaction rate (electrochemical rate) for the 5 samples at 15 and 20 V biases. The experiment measures current, and with a known surface area of electrode it can be converted to current density. The relationship between reaction rate, R and current density J is then:

$$R = \frac{J}{F} \tag{1}$$

Where R is the surface reaction rate expressed in moles $cm^{-2}\,s^{-1}$, J is the current density expressed in amperes (A)-cm^{-2} and F is Faraday's constant, for one electron transfer process [37].

We observed that among the five ionic liquids, $[BMIM]^+[BF_4]^-$ has the highest rate and $[BMIM]^+[PF_6]^-$ the lowest.

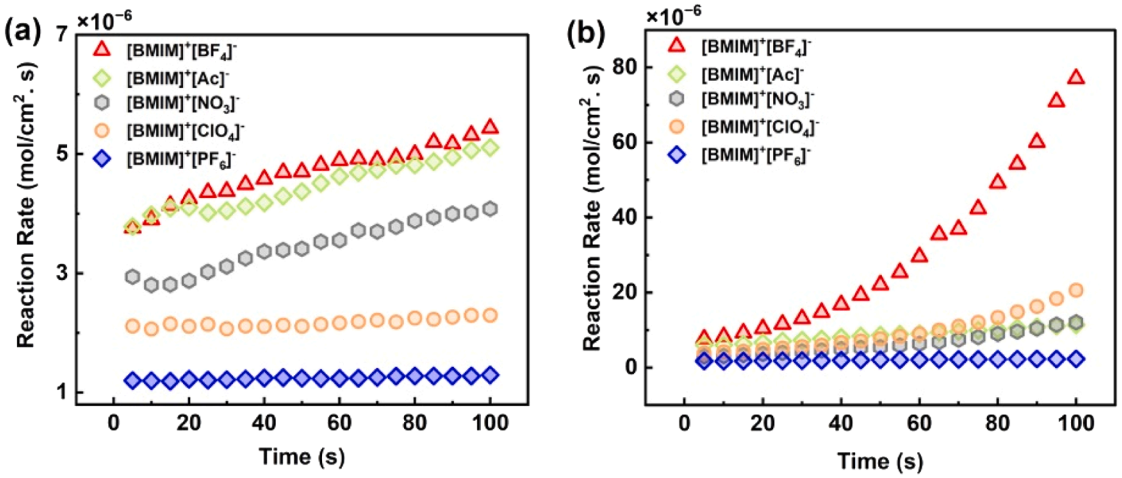

Fig. 5. (a) Reaction rate of RTILs at 15 V (b) reaction rate of RTILs at 20 V.

The measured surface reaction rate is in the order:

$[BMIM]^+[BF_4]^-$ > $[BMIM]^+[Ac]^-$ > $[BMIM]^+[NO_3]^-$ > $[BMIM]^+[ClO_4]^-$ > $[BMIM]^+[PF_6]^-$

The factors that affect the electrode surface reaction rate can be classified in four general categories: external variables (pressure, time), electrical variables (potential, charge), electrolyte variables (temperature, conductivity, flow velocity, bulk concentration) and electrode variables (material, geometry) [38].

The impact of external and electrode variables can be neglected as the same electrode configuration and operating conditions are used for all compounds. Surprisingly, both the highest and lowest reaction rates occurred for the fluorinated anions. From Fig. 4, we see that the difference in the onset oxidation potential between these two is quite small (<0.4 volt), while Fig. 5 demonstrates that the differences in reaction rates can vary significantly, by a factor of 4 at 15 V and up to a factor of 30 at 20 V. An electrochemical reaction at the electrode typically involves multiple steps but can be simplified into two major processes: mass transport associated with drift of ions from the bulk to the electrode surface and electron transfer rate between the electrode and ions [38,39]. Beyond the electrochemical stability window, the I-V current resulting from the second process (Faradic current zone) should show a non-linear Ohmic type behavior resulting from the increase (decrease) of electrode chemical potential with the applied voltage. As we already observed a non-linear current voltage relationship (Fig. 4), dominant effects from the ion to electrode charge transfer can be ruled out [39,40]. Moreover, the similar atomic structure of the two anions (BF_4^- and PF_6^-) of these two ionic liquids, and their very similar stability window, we may conjecture that the electrode kinetics may be quite similar, and that the observed differences in reaction rates for these two RTILs might be attributed to transport properties [41]. In liquids with an active chemical potential gradient, ion-conductivity should dominate over self-diffusivity, and is strongly dependent on the charge carrier concentration, their mobility, Coulombic and van der Waals intermolecular interactions [42–44].According to several literature sources $[BMIM]^+[BF_4]^-$ exhibits higher specific conductivity than $[BMIM]^+[PF_6]^-$ over a range of temperatures [45,46].This is consistent with our observation of electrochemical activity and from available literature $[BMIM]^+[BF_4]^-$ should have the highest ionic conductivity among all the RTILs explored in our work [47,48].

Electrical conductivity of an electrolyte is directly proportional to the density of charge carriers and their mobility [44]. Since we have already seen that the surface reaction rate of the different ionic liquids does not correlate with the redox onset potential and is mostly controlled by mass transfer, the role of carrier concentration can be eliminated [49]. Hence, mobility should be the dominant controller of conductivity which in turn is nominally inversely related to the size of the ion and viscosity of the medium [44,49].

Both molar volume and anion volume of $[BMIM]^+[PF_6]^-$ are larger than those of $[BMIM]^+[BF_4]^-$ [48,50].Additionally, due to greater charge delocalization in PF_6^-, $[BMIM]^+[PF_6]^-$ is known to exhibit a higher viscosity than $[BMIM]^+[BF_4]^-$ [51]. The combination of a larger size and a higher viscosity should result in a lower conductivity. Although NO_3^- has lower anion volume than BF_4^-,the corresponding room temperature imidazole ionic liquid $[BMIM]^+[NO_3]^-$ exhibits lower conductivity than $[BMIM]^+[BF_4]^-$ and we observe a lower reaction rate [47,48,50]. We attribute this to differences in hydrogen bonding with the anion's electronegative element (ion-ion interactions). In particular the H atom on the C2 carbon forms a stronger bond C—H···O than C—H···F [52–54].This should lead to increased viscosity and ion localization which ultimately decreases the conductivity. Although $[BMIM]^+[Ac]^-$ has lower conductivity than $[BMIM]^+[NO_3]^-$ according to the values reported in literature, we observed a slightly increased reaction rate for $[BMIM]^+[Ac]^-$ [47,55]. This could be because $[BMIM]^+[Ac]^-$ is more hygroscopic in nature and its conductivity can increase with enhanced water content as presence of polar impurity overcomes the solvation enthalpy [56,57].

Increasing the bias voltage to 20 V as shown in Fig. 5b results in an increase in reaction rate. $[BMIM]^+[BF_4]^-$ showed the largest effect with an almost 14x increase relative to that at the 15 V near the end of electrolysis. However, $[BMIM]^+[PF_6]^-$ only shows a 1.8x increase. The other ionic liquids, $[BMIM]^+[Ac]^-$, $[BMIM]^+[NO_3]^-$ also exhibited small increases in rate at 20 V compared to 15 V except for $[BMIM]^+[ClO_4]^-$, for which we saw a sudden increase in rate at 20 V.

One of the obvious observations in our experiments is the temporal increase in the electrochemical rate. Ionic Joule heating is a huge challenge for solid and viscous liquid electrolytes due to high density and strong intermolecular forces and hence our experiments are not necessarily isothermal. Indeed, thermal imaging of $[BMIM]^+[BF_4]^-$ with an IR camera as shown in Fig. 6a clearly shows a generally homogenous increase in temperature.

Temporal temperature plots in Fig. 6b for all the RTILs at 15 V clearly show that all the liquids are heating albeit at different rates. $[BMIM]^+[BF_4]^-$ and $[BMIM]^+[Ac]^-$ have the highest temperature rise (~12 °C) over the roughly 100 s of the experiment, while $[BMIM]^+[PF_6]^-$ has a negligible change. In Fig. 6a the spatially homogeneous nature of the temperature rise implies it is not related to any exothermicity at the electrode, but rather should be attributed to dissipative Joule heating and thus related to conductivity. The temperature was averaged over the region between the electrodes for each RTIL (Fig. 6b, c). In the temporal temperature plot for RTILs at 20 V (Fig. 6c), we observe a sudden temperature rise for $[BMIM]^+[ClO_4]^-$ which explains its rise in reaction rate at 20 V.

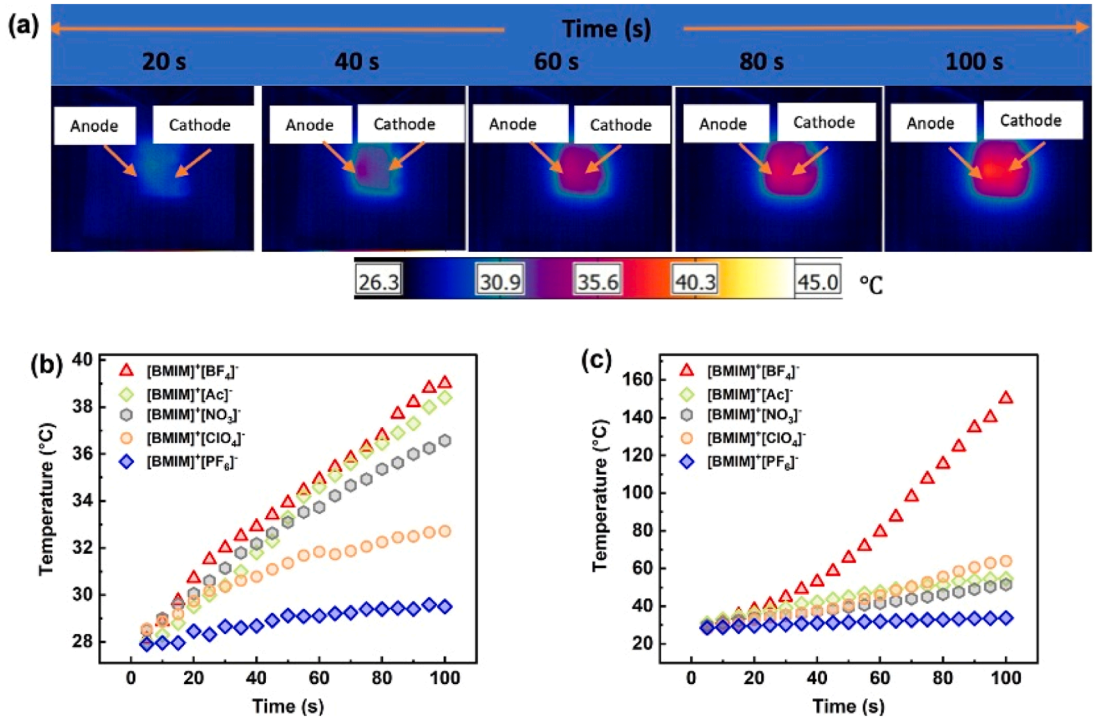

Fig. 6. (a) Temporal IR thermograph of $[BMIM]^+[BF_4]^-$ at 15 V (b) Average temperature of RTILs with time at 15 V (c) Average temperature of RTILs with time at 20 V.

We have already argued that the difference in observed reaction rates is likely due to transport limitations. We now further explore this point through an assessment of temperature dependence of conductivity, in order to explain the temporal rate increases observed, through the Vogel-Fulcher-Tammann (VFT) correlation:

$$\sigma(T) = \sigma_o exp\ \frac{-A}{(T - T_{o,\sigma})} \tag{2}$$

Where is σ is the conductivity and σ_o, A, $T_{o,\sigma}$ are fitting parameters.

To assess if the temporal increase in reaction rate can simply be attributable to the increase in conductivity due to Joule heating, we normalize the experimental reaction rate in Fig. 5, by the estimated temperature dependent conductivity (Eq. (2)) as shown in Fig. 7a, b. The fitting parameters used for conductivity estimation is listed in Table S1 in the supplemental. Unfortunately, parameters were only available for two ionic liquids $[BMIM]^+[BF_4]^-$ and $[BMIM]^+[PF_6]^-$ and no reliable temperature dependent conductivity parameters for the others could be found. As a work around we used the average of the fitting parameters for the remaining ionic liquids. We believe this approach is reasonable because the reported room temperature conductivity values of these three ionic liquids in the literature fall within the range of $[BMIM]^+[BF_4]^-$ and $[BMIM]^+[PF_6]^-$. In Fig. 7 we normalize the temporal variation of reaction rate with the temperature dependent conductivity. Fig. 7a shows that at 15 V, the reaction rate R, normalized by conductivity, σ remains constant over time for all the ionic liquids. This indicates the change in reaction rate observed in Fig. 5 is directly attributable to temperature dependent changes in conductivity which confirms our initial conjecture that this is a transport limited process. However, at 20 V (Fig. 7b), this trend appears not to hold, at least for $[BMIM]^+[BF_4]^-$, where the normalized reaction rate decreases. According to Fig. 5b, $[BMIM]^+[BF_4]^-$ exhibits a substantially higher reaction rate at 20 V compared to other ionic liquids suggesting significant

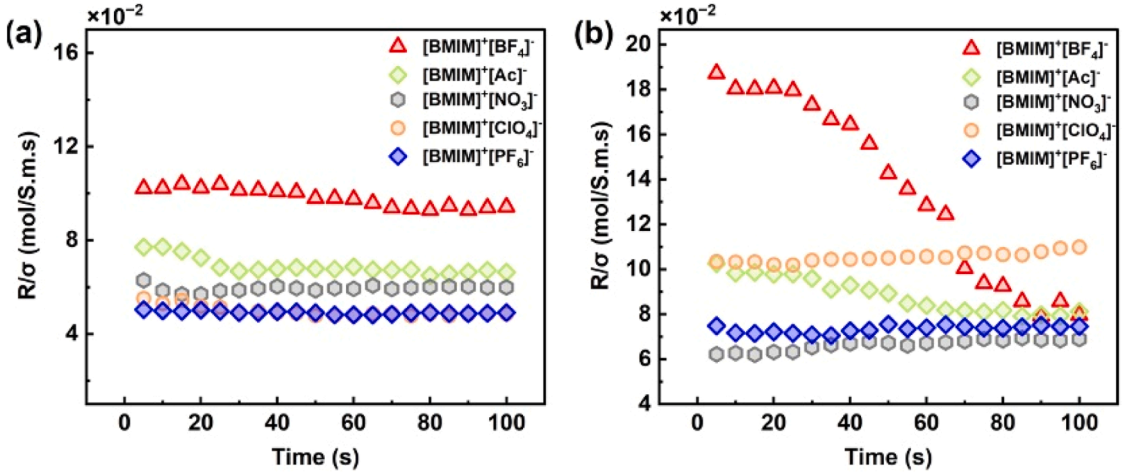

Fig. 7. (a) Normalized reaction rate of RTILs at 15 V (b) normalized reaction rate of RTILs at 20 V.

electrolyte consumption. By analyzing the area under the curve of the temporal current response of the ionic liquids at 20 V, we estimated that approximately 40 % of $[BMIM]^+[BF_4]^-$ was consumed over 100 s of electrolysis, whereas for $[BMIM]^+[PF_6]^-$ the consumption was as low as 3 %. This likely explains the decrease in normalized reaction rate for $[BMIM]^+[BF_4]^-$ at 20 V, as the depletion of reactants near the electrode surface hinders the charge transfer process which higher conductivity cannot fully compensate for. Given the temporal change in reaction rate for $[BMIM]^+[BF_4]^-$ at 20 V (Fig. 7b), an attempted fit to extract a reaction order of the electrochemical reaction shows an initial first order rate by assuming the reaction is elementary initially. Details may be found in supplemental. We also see a decrease in the normalized rate for, $[BMIM]^+[Ac]^-$ at 20 V of about 20 % but given the aforementioned approximation in conductivity we cannot say much about this change. Furthermore, we observed a significant difference between the surface reaction rates between 15 and 20 V for $[BMIM]^+[BF_4]^-$ (Fig. 5a, b), with up to 14-fold increase in rates. However, in Fig. 7a, b, the difference between the normalized reaction rates was not as substantial. The reason behind this is, the up to 110 K difference in temperature between 15 and 20 V cases. Higher temperatures lead to higher conductivity which increased the reaction rates and that the temperature dependance of the rate could be corrected by the Vogel-Fulcher-Tammann (VFT) correlation, implying mass transfer rate control. It also means that the effective activation energy in the system is dominated by the potential barrier to ionic hopping due to strong intermolecular forces which we find to be ~10–11 kJ/mol predicted from the VFT correlation of conductivity.

3.3. Combustion control and electrochemical activity

The extremely low vapor pressure of RTILs is one of the main reasons for considering them non-flammable as discussed previously. Additionally, the aromatic imidazole ring of the room temperature imidazole ionic liquids can remain thermally stable and oxidation resistant, further contributing to their inflammability [58–60]. Similar to $[BMIM]^+[ClO_4]^-$, studied in our previous work, we observed that the other four imidazole ionic liquids in this study are also non-flammable when exposed to an external ignition source [24]. In Fig. S6 in the supplementary section we demonstrated the nonflammability of $[BMIM]^+[NO_3]^-$, as an example when an external ignition source was applied. Fig. 1 illustrates the proposed mechanism by which the cation is reduced resulting in a neutral molecule that is then volatile and flammable. We hypothesize that the ionic liquid with higher surface reaction rate should ignite faster and combust more effectively. Among the five ionic liquids we investigated at 15 V and 20 V, $[BMIM]^+[BF_4]^-$, exhibited the fastest rate and produced the most current. However, surprisingly, we couldn't ignite this ionic liquid upon electrochemical decomposition using an external ignition source. Table 1 presents the combustion behavior and cyclability of the five ionic liquids during electrolysis.

Among the five RTILs, $[BMIM]^+[BF_4]^-$ and $[BMIM]^+[PF_6]^-$ were not combustible, while the remaining three were combustible upon electrochemical decomposition. Their flammability can be modulated by turning the voltage bias on and off as demonstrated in Fig. 3. Additionally, the combustion behavior of the $[BMIM]^+[NO_3]^-$ and $[BMIM]^+[Ac]^-$ are shown in the supplementary section in videos SV1 and SV2.

Table 1
Combustion behavior and cyclability of ionic liquids.

Ionic Liquid	Inherently Flammable?	Electrochemically Flammable?	Flammability cycling?
$[BMIM]^+[BF_4]^-$	No	No	N/A
$[BMIM]^+[CH_3COO]^-$	No	Yes	Yes
$[BMIM]^+[NO_3]^-$	No	Yes	Yes
$[BMIM]^+[ClO_4]^-$	No	Yes	Yes
$[BMIM]^+[PF_6]^-$	No	No	N/A

To investigate why $[BMIM]^+[BF_4]^-$ and $[BMIM]^+[PF_6]^-$ weren't combustible even though they clearly showed electrochemical activity, we analyzed the gaseous species evolved during the electrochemical decomposition of the ionic liquids under vacuum using time-of-flight mass spectrometry. Fig. 8 presents time-of-flight mass spectrometry results for the five ionic liquids at 20 V. Details of the mass spectrometer operation can be found in the experimental section. The time-averaged mass spectra of all five ionic liquids, over 100 ms at a sampling rate of 10 KHz shows characteristic peaks for $BMIM^+$ fragments, 1-butyl 3-methyl imidazole-2-yl radical ([BMIM]•, $m/z = 139$), 1-methyl imidazole-2-yl radical, ([MIM]•, $m/z = 83$), and butene ($m/z = 28, 41, 56$) at 20 V [61,62]. In our previous work we discussed the mechanism of generation of these radicals. In summary, when the $[BMIM]^+$ is reduced, the isomer with the methyl group attached to the N^+ atom of the imidazole ring forms [BMIM]• while the isomer with the butyl group attached to the N+ results in the formation of [MIM]• and butene [24]. From Fig. 8, we observe that gaseous products from oxidation at the anode are also present in the spectra. For $[BMIM]^+[BF_4]^-$ there are two additional peaks at $m/z = 69$ BF_3 and $m/z = 49$ BF_2. In the case of $[BMIM]^+[Ac]^-$ a prominent peak at $m/z = 44$ corresponds to CO_2 from acetate oxidation and another peak at $m/z = 45$, which we attribute to COOH [63]. For $[BMIM]^+[NO_3]^-$ we see a new peak at $m/z = 46$ which we believe is NO_2 from nitrate oxidation. Lastly for $[BMIM]^+[PF_6]^-$ we observe PF_4 at $m/z = 107$, PF_3 at $m/z = 88$, PF_2 at $m/z = 69$ and PF at $m/z = 50$. The possible corresponding anodic reactions are listed in Table 2.

We believe the presence of halogenated boron and phosphorous gaseous products from the oxidation of BF_4^- and PF_6^- anions respectively, likely act as flame retardants [70,71].As shown in Fig. 8, both ionic

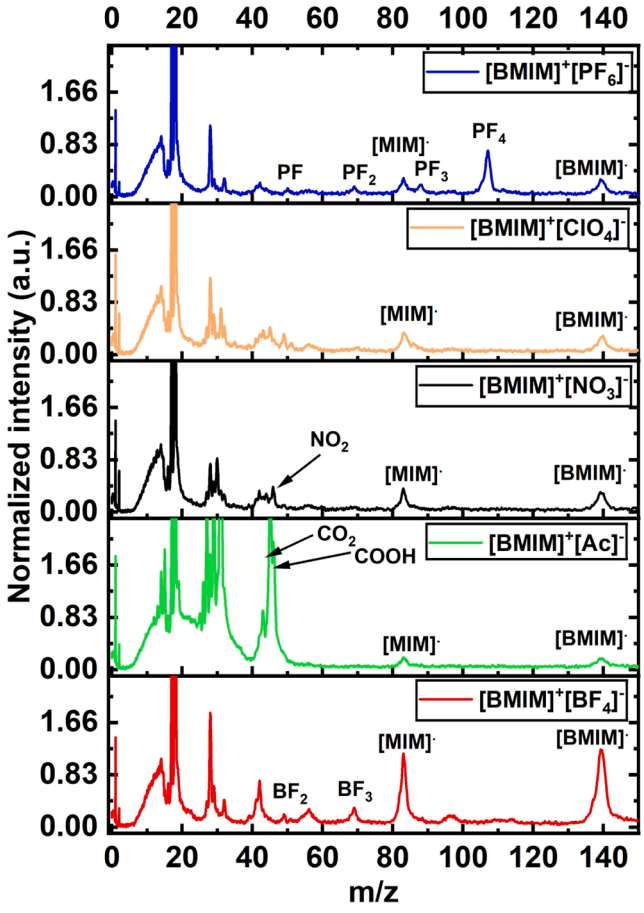

Fig. 8. Time of fight mass spectrometry of ionic liquids at 20 V.

Table 2
Possible reactions of the ionic liquids at the anode.

Ionic Liquid	Anode Reaction	Refs.
$[BMIM]^+[BF_4]^-$	$BF_4^- \rightarrow BF_3 + F_{ads} + e^-$	[63]
$[BMIM]^+[Ac]^-$	$CH_3COO^- \rightarrow CO_2 + H_2O + e^-$	[64]
$[BMIM]^+[NO_3]^-$	$NO_3^- \rightarrow NO_2 + ½O_2 + e^-$	[65]
$[BMIM]^+[ClO_4]^-$	$ClO_4^- \rightarrow ClO_3^- + O_{ads} + e^-$	[66–68]
$[BMIM]^+[PF_6]^-$	$PF_6^- \rightarrow PF_5 + F_{ads} + e^-$	[69]

liquids contain fluorinated compounds resulting from anion oxidation in the gas phase. These fluorinated compounds can scavenge radicals (O, H, OH) necessary to propagate chain reaction processes required for combustion, thereby acting as inhibitors [72]. In the case of $[BMIM]^+[PF_6]^-$ the gas phase contains both phosphorous and fluorine and both are known to act as gas phase inhibitors [73,74]. We conclude that although $[BMIM]^+[BF_4]^-$ and $[BMIM]^+[PF_6]^-$ generate reactive gaseous species upon reduction at the cathode, they cannot be ignited due to the flame-retardant properties of the halogenated anodic products. Among the other three electrochemically flammable RTILs, $[BMIM]^+[Ac]^-$ is the most suitable fuel at low voltage due to its higher rate of gaseous species generation and $[BMIM]^+[ClO_4]^-$ is the best choice at high voltage for the same reason.

4. Conclusions

In this study, we explore the role of anions in RTILs that can be employed to modulate combustion by electrochemical means. In this way seemingly nonflammable fuels can be activated by application of voltage bias. Through electrochemical measurement, we estimated the rate of volatile flammable gaseous species generation of five ionic liquids. Contrary to classical isothermal reactions, where the consumption of reactants leads to a decrease in rates, we observed an increase in rates for all five ionic liquids. IR imaging revealed that our system is not isothermal with each of the five ionic liquids heating up at different rates. Since conductivity typically defines the transport process for highly ionic systems, we expected that ionic liquid with higher conductivity would have a higher rate of gaseous species production. Indeed, we found that $[BMIM]^+ [BF_4]^-$, the ionic liquid with the highest conductivity, exhibited the highest rate of gaseous species production. Additionally, we predicted the change in conductivity with temperature using Vogel-Fulcher-Tammann (VFT) correlation. To support our hypothesis that the increase in temporal rate is due to temperature dependent conductivity, we normalized the rates for all ionic liquids by their conductivity at the corresponding temperature. We found that the rates remained mostly constant, with few exceptions reinforcing our conjecture that our system is limited by mass transport. While we initially expected that the combustion behavior would largely depend on the quantity of gaseous species generated — the more gaseous species, the better the combustion, our study revealed that, the anion plays a critical role in determining the flammability of the ionic liquid. Despite generating the highest amount of reactive gaseous species, an ionic liquid can remain non-flammable due to the hindrance caused by its anion. Mass spectrometric analysis demonstrated that the flame-inhibiting properties of the gaseous species generated from the anion oxidation at the anode can interfere with the flammability of the gaseous species generated at the cathode, regardless of the ionic liquid's ability to produce reactive species at a high rate. To determine which ionic liquid has the potential to be used as a 'safe' fuel where its flammability can be controlled by electrochemical means, we need to evaluate the contribution of the anion of that room temperature imidazole ionic liquid.

Novelty and significance statement

Room temperature ionic liquids (RTILs) are usually considered non-flammable owing to their extremely low vapor pressure and superior thermal stability. However, most RTILs possess high energy density. RTILs with metastable anions can decompose thermally and hypergolically to reactive flammable species but RTILs without these anions need other ways to produce reactive species. Previous study has shown that an apparent non-flammable RTIL can be made flammable 'electrochemically' and its flammability can be controlled by toggling the applied voltage. However, the effects of anions on the electrochemical modulation of flammability of RTILs have not been studied. This study shows that the electrochemical modulation of flammability of RTILs largely depends on the anions. Despite generating reactive gaseous species through cathodic reduction, some RTILs can still be non-flammable if the anodic oxidation products possess flame inhibition properties. Flammability of the RTILs without such anodic oxidation products can be modulated electrochemically.

CRediT authorship contribution statement

Afrida Anis: Writing – original draft, Data curation, Conceptualization, Investigation. **Keren Shi:** Writing – review & editing, Data curation. **Erik Hagen:** Visualization, Data curation. **Yujie Wang:** Visualization, Data curation. **Prithwish Biswas:** Writing – review & editing, Formal analysis. **Michael R. Zachariah:** Writing – review & editing, Supervision, Resources, Project administration, Methodology, Investigation, Funding acquisition, Formal analysis, Conceptualization.

Declaration of competing interest

On behalf of all the authors, we declare no conflict of interest. This work is original and has not been considered for publication elsewhere.

Supplementary materials

Supplementary material associated with this article can be found, in the online version, at doi:10.1016/j.combustflame.2025.113994.

References

[1] M. Nakamura, F. Akamatsu, R. Kurose, M. Katsuki, Combustion mechanism of liquid fuel spray in a gaseous flame, Phys. Fluids 17 (2005) 123301.
[2] D.B. Spalding, Combustion of liquid fuels, Nature 165 (1950) 160.
[3] D.A. Saldana, L. Starck, P. Mougin, B. Rousseau, B. Creton, Prediction of flash points for fuel mixtures using machine learning and a novel equation, Energy Fuels. 27 (2013) 3811–3820.
[4] B. Gobin, N. Harvey, G. Young, Combustion characteristics of electrically controlled solid propellants using polymer electrolytes, Combust. Flame 244 (2022) 112291.
[5] I.V. Khoruzhii, G.F. Klyakin, V.A. Taranushich, V.I. Lachin, A study of the electrothermal method for control over combustion velocity under atmospheric pressure of energetic condensed systems based on ammonium nitrate, Russ. J. Appl. Chem. 80 (2007) 1295–1299.
[6] I.V. Khoruzhii, G.F. Klyakin, V.A. Taranushich, V.I. Lachin, Electrothermal method for controlling the ballistic characteristics of energetic condensed systems based on ammonium nitrate, Russ. J. Appl. Chem. 81 (2008) 61–66.
[7] J.E. Bara, D.E. Camper, D.L. Gin, R.D. Noble, Room-temperature ionic liquids and composite materials: platform technologies for CO2 capture, Acc. Chem. Res. 43 (2010) 152–159.
[8] M. Bier, S. Dietrich, Vapour pressure of ionic liquids, Mol. Phys. 108 (2010) 211–214.
[9] H. Tokuda, S. Tsuzuki, Md.A.B.H. Susan, K. Hayamizu, M. Watanabe, How ionic are room-temperature ionic liquids? An indicator of the physicochemical properties, J. Phys. Chem. B 110 (2006) 19593–19600.
[10] C.-C. Chen, H.-J. Liaw, Y.-N. Chen, Flammability characteristics of ionic liquid 1-Decyl-3-methylimidazolium bis(trifluoromethylsulfonyl)imide, J. Loss Prev. Process Ind. 49 (2017) 620–629.
[11] D. Fox, J. Gilman, A. Morgan, J. Shields, P. Maupin, R. Lyon, H. De Long, P. Trulove, Flammability and thermal analysis characterization of imidazolium-based ionic liquids, Ind. Eng. Chem. Res. 47 (2008) 6327–6332.
[12] H. Sun, G. Zhu, X. Xu, M. Liao, Y.-Y. Li, M. Angell, M. Gu, Y. Zhu, W.H. Hung, J. Li, Y. Kuang, Y. Meng, M.-C. Lin, H. Peng, H. Dai, A safe and non-flammable sodium metal battery based on an ionic liquid electrolyte, Nat. Commun. 10 (2019) 3302.
[13] Q. Yang, Z. Zhang, X.-G. Sun, Y.-S. Hu, H. Xing, S. Dai, Ionic liquids and derived materials for lithium and sodium batteries, Chem. Soc. Rev. 47 (2018) 2020–2064.

[14] W.A. van Schalkwijk, B. Scrosati, 2024 Advances in lithium-ion batteries, n.d (2002).
[15] G.A. Giffin, Ionic liquid-based electrolytes for "beyond lithium" battery technologies, J. Mater. Chem. A Mater. 4 (2016) 13378–13389.
[16] M. Smiglak, A. Metlen, R.D. Rogers, The second evolution of ionic liquids: from solvents and separations to advanced materials—energetic examples from the ionic liquid cookbook, Acc. Chem. Res. 40 (2007) 1182–1192.
[17] X. Zhang, L. Pan, L. Wang, J.-J. Zou, Review on synthesis and properties of high-energy-density liquid fuels: hydrocarbons, nanofluids and energetic ionic liquids, Chem. Eng. Sci. 180 (2017) 95–125.
[18] G. Yue, S. Hong, S.-H. Liu, Process hazard assessment of energetic ionic liquid with kinetic evaluation and thermal equilibrium, J. Loss. Prev. Process. Ind. 81 (2023) 104972.
[19] Q. Zhang, J.M. Shreeve, Energetic ionic liquids as explosives and propellant fuels: a new journey of ionic liquid chemistry, Chem. Rev. 114 (2014) 10527–10574.
[20] M. Smiglak, W.M. Reichert, J.D. Holbrey, J.S. Wilkes, L. Sun, J.S. Thrasher, K. Kirichenko, S. Singh, A.R. Katritzky, R.D. Rogers, Combustible ionic liquids by design: is laboratory safety another ionic liquid myth? Chem. Commun. (2006) 2554–2556.
[21] H.-J. Liaw, Y.-R. Liou, P.-H. Liu, H.-Y. Chen, C.-M. Shu, Increased flammability hazard when ionic liquid [C6mim][Cl] is exposed to high temperatures, J. Hazard. Mater. 367 (2019) 407–417.
[22] H.-J. Liaw, C.-C. Chen, Y.-C. Chen, J.-R. Chen, S.-K. Huang, S.-N. Liu, Relationship between flash point of ionic liquids and their thermal decomposition, Green Chem. 14 (2012) 2001–2008.
[23] Y. Zhang, H. Gao, Y.-H. Joo, J.M. Shreeve, Ionic liquids as hypergolic fuels, Angew. Chem. Int. Ed. 50 (2011) 9554–9562.
[24] P. Biswas, Y. Wang, E. Hagen, M.R. Zachariah, Electrochemical modulation of the flammability of ionic liquid fuels, J. Am. Chem. Soc. 145 (2023) 16318–16323.
[25] K.N. Marsh, J.A. Boxall, R. Lichtenthaler, Room temperature ionic liquids and their mixtures—a review, Fluid. Phase Equilib. 219 (2004) 93–98.
[26] A. Paul, S. Muthukumar, S. Prasad, Review—room-temperature ionic liquids for electrochemical application with special focus on gas sensors, J. Electrochem. Soc. 167 (2020) 037511.
[27] A.J. Bard, L.R. Faulkner, H.S. White, Electrochemical Methods: Fundamentals and Applications, Wiley, 2022. https://books.google.com/books?id=eZ6HDAEACAAJ.
[28] L. Zhou, N. Piekiel, S. Chowdhury, M.R. Zachariah, T-Jump/time-of-flight mass spectrometry for time-resolved analysis of energetic materials, Rapid Commun. Mass Spectrom. 23 (2009) 194–202.
[29] G. Jian, L. Zhou, N.W. Piekiel, M.R. Zachariah, Low effective activation energies for oxygen release from metal oxides: evidence for mass-transfer limits at high heating rates, Chemphyschem 15 (2014) 1666–1672.
[30] M. Armand, F. Endres, D.R. MacFarlane, H. Ohno, B. Scrosati, Ionic-liquid materials for the electrochemical challenges of the future, Nat. Mater. 8 (2009) 621–629.
[31] F. Scholz, 2024 Electroanalytical methods guide to experiments and applications 2nd, revised and extended edition 12 3, n.d (2014).
[32] A.R. Harris, D.B. Grayden, S.E. John, Electrochemistry in a two- or three-electrode configuration to understand monopolar or bipolar configurations of platinum bionic implants, Micromachines (Basel) 14 (2023) 722.
[33] S. Kazemiabnavi, Z. Zhang, K. Thornton, S. Banerjee, Electrochemical stability window of imidazolium-based ionic liquids as electrolytes for lithium batteries, J. Phys. Chem. B 120 (2016) 5691–5702.
[34] E. Rogers, B. Sljukic Paunkovic, C. Hardacre, R. Compton, Electrochemistry in room-temperature ionic liquids: potential windows at mercury electrodes, J. Chem. Eng. Data 54 (2009) 2049–2053.
[35] T.L. Greaves, A. Weerawardena, C. Fong, I. Krodkiewska, C.J. Drummond, Protic ionic liquids: solvents with tunable phase behavior and physicochemical properties, J. Phys. Chem. B 110 (2006) 22479–22487.
[36] Q. Li, J. Jiang, G. Li, W. Zhao, X. Zhao, T. Mu, The electrochemical stability of ionic liquids and deep eutectic solvents, Sci. China Chem. 59 (2016) 571–577.
[37] Modern Electrochemistry Second Edition Ionics, n.d (1998).
[38] F.C. Walsh, The kinetics of electrode reactions: part I—general considerations and electron transfer control, Trans. IMF 70 (1992) 50–54.
[39] W.J. Albery, G.B.R. Feilden, G.T. Rogers, W.J. Albery, Electrode kinetics, philosophical transactions of the royal society of London. Series A, Math. Phys. Sci. 302 (1997) 221–235.
[40] C.H. Bamford, C.F.H. Tipper†, R.G. Compton, Electrode Kinetics: Principles and Methodology, Elsevier Science, 1986. https://books.google.com/books?id=wFwjWhRPuR8C.
[41] P.A.Z. Suarez, S. Einloft, J.E.L. Dullius, R.F. de Souza, J. Dupont, Synthesis and physical-chemical properties of ionic liquids based on 1-n-butyl-3-methylimidazolium cation, J. Chim. Phys. 95 (1998) 1626–1639, https://doi.org/10.1051/jcp:1998103.
[42] P. Hapiot, C. Lagrost, Electrochemical reactivity in room-temperature ionic liquids, Chem. Rev. 108 (2008) 2238–2264.
[43] G. Yu, D. Zhao, L. Wen, S. Yang, X. Chen, Viscosity of ionic liquids: database, observation, and quantitative structure-property relationship analysis, AIChE J 58 (2012) 2885–2899.
[44] J. Koryta, J. Dvořák, L. Kavan, Principles of Electrochemistry, Wiley, 1993.
[45] A. Stoppa, O. Zech, W. Kunz, R. Buchner, The conductivity of imidazolium-based ionic liquids from (−35 to 195) °C. A. Variation of cation's alkyl chain, J. Chem. Eng. Data 55 (2010) 1768–1773.
[46] O. Zech, A. Stoppa, R. Buchner, W. Kunz, The conductivity of imidazolium-based ionic liquids from (248 to 468) K. B. Variation of the anion, J. Chem. Eng. Data 55 (2010) 1774–1778.
[47] E.P. Grishina, L.M. Ramenskaya, M.S. Gruzdev, O.V. Kraeva, Water effect on physicochemical properties of 1-butyl-3-methylimidazolium based ionic liquids with inorganic anions, J. Mol. Liq. 177 (2013) 267–272.
[48] S.A. Pandit, M.A. Rather, S.A. Bhat, G.M. Rather, M.A. Bhat, Influence of the anion on the equilibrium and transport properties of 1-butyl-3-methylimidazolium based room temperature ionic liquids, J. Solution. Chem. 45 (2016) 1641–1658.
[49] A. Kokorin, Ionic liquids: theory, properties, new approaches, IntechOpen, 2011. https://books.google.com/books?id=Ky2RDwAAQBAJ.
[50] J.N. Gayton, S. Autry, R.C. Fortenberry, N.I. Hammer, J.H. Delcamp, Counter anion effect on the photophysical properties of emissive indolizine-cyanine dyes in solution and solid state, Molecules 23 (2018) 3051.
[51] A. Stoppa, O. Zech, W. Kunz, R. Buchner, The conductivity of imidazolium-based ionic liquids from (−35 to 195) °C. A. Variation of cation's alkyl chain, J. Chem. Eng. Data 55 (2010) 1768–1773.
[52] K. Dong, S. Zhang, J. Wang, Understanding the hydrogen bonds in ionic liquids and their roles in properties and reactions, Chem. Commun. 52 (2016) 6744–6764.
[53] K. Dong, Y. Song, X. Liu, W. Cheng, X. Yao, S. Zhang, Understanding structures and hydrogen bonds of ionic liquids at the electronic level, J. Phys. Chem. B 116 (2012) 1007–1017.
[54] K. Fumino, A. Wulf, R. Ludwig, The potential role of hydrogen bonding in aprotic and protic ionic liquids, Phys. Chem. Chem. Phys. 11 (2009) 8790–8794.
[55] A. Xu, Y. Zhang, Z. Li, J. Wang, Viscosities and conductivities of 1-butyl-3-methylimidazolium carboxylates ionic liquids at different temperatures, J. Chem. Eng. Data 57 (2012) 3102–3108.
[56] K.R. Seddon, A. Stark, M.-J. Torres, Influence of chloride, water, and organic solvents on the physical properties of ionic liquids, 72 (2000) 2275–2287.
[57] Y. Cao, Y. Chen, X. Sun, Z. Zhang, T. Mu, Water sorption in ionic liquids: kinetics, mechanisms and hydrophilicity, Phys. Chem. Chem. Phys. 14 (2012) 12252–12262.
[58] L. Zhao, S.B. Li, G.A. Wen, B. Peng, W. Huang, Imidazole derivatives: thermally stable organic luminescence materials, Mater. Chem. Phys. 100 (2006) 460–463.
[59] H.-T. Kim, J. Kang, J. Mun, S.M. Oh, T. Yim, Y.G. Kim, Pyrrolinium-based ionic liquid as a flame retardant for binary electrolytes of lithium ion batteries, ACS Sustain. Chem. Eng. 4 (2016) 497–505.
[60] W.-T. Wang, S.-H. Liu, Y. Wang, C.-F. Yu, Y.-F. Cheng, C.-M. Shu, Thermal stability and exothermic behaviour of imidazole ionic liquids with different anion types under oxidising and inert atmospheres, J. Mol. Liq. 343 (2021) 117691.
[61] P.J. Linstrom, W.G. Mallard, Eds. 2024 NIST chemistry WebBook, NIST standard reference database number 69, (n.d.) (2011).
[62] A. Deyko, K.R.J. Lovelock, P. Licence, R.G. Jones, The vapour of imidazolium-based ionic liquids: a mass spectrometry study, Phys. Chem. Chem. Phys. 13 (2011) 16841–16850.
[63] A.M. Andersson, M. Herstedt, A.G. Bishop, K. Edström, The influence of lithium salt on the interfacial reactions controlling the thermal stability of graphite anodes, Electrochim. Acta 47 (2002) 1885–1898.
[64] K. Obileke, H. Onyeaka, E. Meyer, N. Nwokolo, Microbial fuel cells, a renewable energy technology for bio-electricity generation: a mini-review, Electrochem. Commun. 125 (2021) 107003.
[65] T.L. Broder, D.S. Silvester, L. Aldous, C. Hardacre, A. Crossley, R.G. Compton, The electrochemical oxidation and reduction of nitrate ions in the room temperature ionic liquid [C2mim][NTf2]; the latter behaves as a 'melt' rather than an 'organic solvent, New J. Chem. 31 (2007) 966–972.
[66] M.H. Miles, A.N. Fletcher, The electrochemical reduction of molten perchlorate and chlorate salts, J. Electrochem. Soc. 128 (1981) 821.
[67] Y.J. Jung, K.W. Baek, B.S. Oh, J.-W. Kang, An investigation of the formation of chlorate and perchlorate during electrolysis using Pt/Ti electrodes: the effects of pH and reactive oxygen species and the results of kinetic studies, Water Res. 44 (2010) 5345–5355.
[68] J.-J. Li, M.-M. Gao, G. Zhang, X.-H. Wang, S.-G. Wang, C. Song, Y.-Y. Xu, Perchlorate reduction in microbial electrolysis cell with polyaniline modified cathode, Bioresour. Technol. 177 (2015) 74–79.
[69] Y. Liu, K. Xie, Y. Pan, Y. Li, W. Lu, S. Liu, C. Zheng, Impacts of lithium tetrafluoroborate and lithium difluoro(oxalate)borate as additives on the storage life of Li-ion battery at elevated temperature, Ionics (Kiel) 24 (2018) 1617–1628.
[70] M.A. Kasem, H.R. Richards, Flame-retardants for fabrics. Function of boron-containing additives, Product. R&D 11 (1972) 114–133.
[71] A. Granzow, Flame retardation by phosphorus compounds, Acc. Chem. Res. 11 (1978) 177–183.
[72] X. Mu, H. Cong, Z. Shao, Z. Yuan, B. Zhu, K. Zhang, M. Bi, X. Wang, Experimental and theoretical research on the inhibition performance of ethanol gasoline/air explosion by C6F12O, J. Loss. Prev. Process. Ind. 83 (2023) 105088.
[73] L. Wang, L. Li, Q. Fan, T. Chu, Y. Wang, Y. Xu, Thermal stability and flammability of several quaternary ammonium ionic liquids, J. Mol. Liq. 382 (2023) 121920.
[74] D.M. Fox, J.W. Gilman, A.B. Morgan, J.R. Shields, P.H. Maupin, R.E. Lyon, H.C. De Long, P.C. Trulove, Flammability and thermal analysis characterization of imidazolium-based ionic liquids, Ind. Eng. Chem. Res. 47 (2008) 6327–6332.